Dual-driven Learning for RIS-assisted Multi-user MISO Beamforming and Reflection with Uplink Channel Information

Kai Liang, Member, IEEE, Ruihua Zhang, Gan Zheng, Fellow, IEEE, and Kai-Kit Wong, Fellow, IEEE

Abstract—Reconfigurable intelligent surface (RIS) can improve wireless transmission performance by passive reflective elements to reconfigure the wireless propagation environment. However, the traditional optimization approach has a high complexity when jointly optimizing phase shifts at the RIS and the beamforming at the base station (BS). This paper focuses on the sum rate maximization problem with the transmit power constraint and the phase constraint, for the RIS-assisted multiuser multipleinput-single-output (MISO) downlink transmission where the downlink and uplink channel reciprocity does not exist. To solve this problem, we propose a data and model-driven learning approach via a hybrid learning manner. Specifically, we adopt an optimal beamforming structure to effectively reduce the output dimension and to improve the training and testing efficiency of the neural network. Then, we provide a learning framework including several fully-connected neural networks to learn the mapping between uplink and downlink channels, power features of the beamforming, and phase-shift matrices, after which the optimal beamforming can be recovered by the proposed beamforming structure. Simulation results show that our proposed method achieves better rate performance than state-of-the-art data-driven learning approaches.

 ${\it Index~Terms} {\color{red}\textbf{—}} RIS, deep \ learning, multiuser \ MISO, beamforming.$

I. INTRODUCTION

Reconfigurable intelligent surface (RIS) [1]–[3], utilizes a set of passive radio elements to flexibly adjust the reflection of incident signals, thereby improving the rate, spectral efficiency, coverage, and other performance of the communication system. Considering its ability to enhance the performance of communication systems and the low power consumption

Copyright (c) 20xx IEEE. Personal use of this material is permitted. However, permission to use this material for any other purposes must be obtained from the IEEE by sending a request to pubs-permissions@ieee.org. This work was supported in part by the Key Research and Development Program of Shaanxi (2024GX-YBXM-019), in part by Open Fund of Anhui Province Key Laboratory of Cyberspace Security Situation Awareness and Evaluation (CSSAE-2023-007). (Corresponding author: Kai Liang.)

- K. Liang is with the School of Telecommunications Engineering, Xidian University, Xian 710071, China, and also with the Anhui Province Key Laboratory of Cyberspace Security Situation Awareness and Evaluation, Hefei 230037, China (email: kliang@xidian.edu.cn).
- R. Zhang is with the School of Telecommunications Engineering, Xidian University, Xi'an, 710071, China (email: 22011210984@stu.xidian.edu.cn).
- G. Zheng is with the School of Engineering, University of Warwick, Coventry, CV4 7AL, UK (email: gan.zheng@warwick.ac.uk).
- K.-K. Wong is with the Department of Electronic and Electrical Engineering, University College London, London, WC1E 6BT, UK (email: kai-kit.wong@ucl.ac.uk). He is also afliated with Yonsei Frontier Lab., Yonseu University, Seoul, 03722, Korea.

of passive radio elements, RIS has gained wide attention and has been used to various applications, such as device-to-device communications [4], [5], heterogeneous networks [6], [7], simultaneous wireless information and power transmission [8], [9], and unmanned aerial vehicle networks [10], [11].

This paper focuses on the RIS-assisted multiuser multipleinput-single-output (MISO) downlink transmission, and investigates the joint optimal design of beamforming at the base station (BS) and phase-shifts of passive radio elements at the RIS. This is a very challenging work because the optimization problems (e.g., the classical rate maximization problem with power and continuous or discrete phase constraints) are usually non-convex. Traditionally, the joint beamforming and continuous phase optimization problem can be solved by the alternating optimization [12] or its variants block coordinate descent (BCD) [13]-[15], and semidefinite relaxation(SDR) [16], [17]. By applying SDR and alternating optimization techniques, [18] proposes an efficient algorithm to jointly optimize the active transmit beamforming of the AP and the passive reflective beamforming of the RIS. In [19], the joint optimization problem is decomposed into two sub-problems (namely, the conventional BS beamforming design problem and the continuous phase optimization problem), which are solved by the BCD method. Contrary to its assumption of continuous phase shifts, [20], [21] consider the practical case where each element of the RIS has only a finite number of discrete phase shifts. [20] proposes a successive refinement algorithm to optimize the RIS discrete phase shifts for a singleuser setup, and then extends the algorithm to the general case of multiple users. However, these iterative algorithms suffer from high complexity and slow convergence speed, which limits its adoption in 5G or 6G systems, especially for some delay-sensitive services. In addition, existing literature performs joint optimization of beamforming and phase shifts in different frequency bands and specific configurations. Among them, [25] explores the joint optimization of spectrum, coding and phase-shifting in terahertz communication systems, while [26] focuses on RIS-assisted phase optimization in single-input single-output (SISO) systems. [27] proposes signal focusing via phase shifting of RIS in indoor scenarios. While these studies provide important theoretical foundations, most of them do not adequately consider the case of missing upstream and downstream channel reciprocity, especially in RIS-assisted multiuser multiple-input-multiple-output (MU-MISO) systems in frequency bands below 6G.

Recently, the success of deep learning has opened up a

1

tractable "learn to optimize" approach to solving traditional optimization problems [28]–[30]. [28] studies the beamforming problem from a data-driven perspective and, in particular, proposes a multilayer fully connected neural network (FCNN) to learn the phase shift of a single-user system in order to reduce the complexity of the algorithms executed to optimize RIS. In [29], the authors adopt a graph neural network (GNN) architecture to model the interactions between multiple users in a RIS system to directly learn the beamforming for the BS and the reflection phase for the RIS. [30] proposes a fully distributed machine learning algorithm where each BS can locally design its beamforming vectors, and the RIS reflection coefficients are determined by one of the BSs. Nevertheless, the neural networks in all these works are learned in a datadriven manner, which requires a large number of samples to train thus reducing the speed of convergence and accuracy of training.

A natural idea to address this shortcoming is to reduce the output of the neural network by introducing classical models from wireless communication theory, i.e., using a modeldriven learning approach. A lot of previous work has focused on the optimization of beamforming in multiuser MISO. In our previous work [31], a model-driven deep learning approach is proposed for beamforming in multiuser MISO downlink transmissions, where the neural network learns the power feature instead of beamforming vectors by adopting an optimal beamforming structure [32]. This approach reduces the output dimension and improves transmission performance, thus being widely extended in [33]-[35]. However, in RIS-assisted MISO systems, beamforming and phase-shift optimization are coupled with each other, which is very challenging for modeldriven learning methods. In [36], the authors propose a joint beamforming and phase-shift optimization method based on model-driven and GNN, obtaining low complexity and better performance. The inputs to the neural network include CSI from base station to users, from base station to RIS, and from RIS to users. However, the passive elements of the RIS are not able to actively send and receive signals, so it is a challenge to estimate the channel state information from the base station to the RIS and from the RIS to the users.

Another readily overlooked issue is that the reciprocity between the uplink and the downlink channels may not exist. Wireless channel state information (CSI) is critical for beamfoming in multiuser multi-antenna system, providing key information about channel quality and environmental conditions [37], [38]. Most existing works assume that perfect CSI is available at the BS, which can estimate the CSI of the downlink from the pilots transmitted by the mobile user in the uplink. However, this approach is based on the assumption that channel reciprocity conditions exist. In practice, the presence of the analog front-end circuitry in actual radio units complicates the situation and makes the baseband-to-baseband channel non-reciprocal [39], [40]. In [41], we extend the model-driven learning approach in [31] for multiuser MISO with the consideration of only uplink CSI being available at the BS, where the linear channel model [42] is used to describe the relationship between the downlink and uplink channels. This motivates us to use a similar method to deal with this issue.

Based on the above observations, this paper provides a data- and model-driven, i.e., dual-driven, approach to solve the joint optimization problem of beamforming and reflection for the RIS-assisted multi-user MISO system. We focus on the sum rate maximization problem while satisfying the transmit power constraint at the BS and continuous or discrete phase constraints at the RIS, where the BS only knows the uplink CSI. To the best of our knowledge, this is the first work that jointly considers the model-driven learning and the absence of reciprocity between the uplink and the downlink channels in the RIS-assisted multiuser MISO system. The contributions of this paper are summarized as follows.

- We propose a dual-driven learning approach. We first provide the optimal beamforming structure for the RISassisted MISO system, which is based on the phase-shift vector, and the equivalent downlink channel that includes the direct channel from the BS to users, and the cascade channel from the BS to RIS and then to users. Then, we propose an overall deep neural network consisting of four sub-networks to respectively learn the downlink direct and cascade CSI, the phase vector, and power features, which are used to recover the beamforming matrix via the aforementioned optimal beamforming structure. The proposed neural network is trained in a hybrid learning manner. Specifically, the downlink CSI, phase-shifts and power feature are learned in a supervised manner, and the sum rate is learned in an unsupervised manner. The overall loss function is chosen to be a weighted sum of four sub-nets' loss function.
- We use the uplink channel information to learn the down-link channel and the reflection phase shift. Specifically, we assume that there exists a deterministic unique mapping from the uplink channel to the downlink channel, which can be learned by a deep neural network. Similarly, the mapping between the uplink channel information and the optimal phase-shift can be learned via another neural network in a supervised manner.
- We conduct a large number of simulations to evaluate the performance of the proposed algorithm, and these experimental results fully validate the effectiveness and excellent performance of our algorithm. Compared with traditional methods, our algorithm shows significant advantages in improving the total system rate, and it is also able to achieve satisfactory results close to state-of-the-art numerical algorithms with perfect CSI.

The rest of this paper are organized as follows. The system model is presented in Section II. Section III describes the dual-driven learning method for joint optimization of beamforming and reflection. Numerical results and analysis are given in Section IV, after which we conclude this paper in Section V.

Notation: Bold lowercase and capital letters are used to represent column vectors and matrices, respectively. We use $[\mathbf{A}]_{ij}$ and $[\mathbf{a}]_i$ to denote the element of the matrix \mathbf{A} in i-th row and j-th column, and the i-th element of the vector \mathbf{a} , respectively. $(\cdot)^{\mathrm{T}}$ and $(\cdot)^{\mathrm{H}}$ denote the transpose and the conjugate transpose of matrix, respectively. $\mathcal{CN}(\mu, \sigma^2)$ rep-

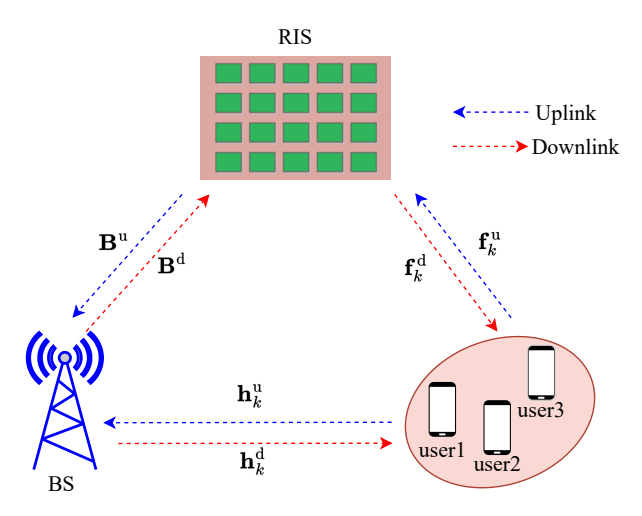


Fig. 1: RIS-assisted multi-user MISO system

resents a complex Gaussian distribution with mean μ and variance σ^2 . $|\cdot|$ and $\|\cdot\|$ refer to the absolute value operator and the Euclidean norm operator, respectively. We use $\operatorname{diag}(\cdot)$ to denote the diagonal matrix of the elements. $\mathbb{R}^{m\times n}$ and $\mathbb{C}^{m\times n}$ are respectively the real and complex spaces of m by n dimensions. $\operatorname{mod}(b,m)$ returns the remainder of b divided by m. $\lfloor \cdot \rfloor$ denotes the floor function (i.e. a downward rounding operation).

II. SYSTEM MODEL AND PROBLEM FORMULATION

A. System Model

We start with a RIS-assisted downlink multi-user MISO system, where a BS with N antennas serves K single-antenna users. A RIS equipped with M passive reflective elements is used to assist transmission between the BS and the users. By adjusting the phase of elements, incident signals are reflected to the users in the desired direction as shown in Fig. 1. Let $\mathbf{h}_k^{\mathrm{d}} \in \mathbb{C}^{1 \times N}$, $\mathbf{f}_k^{\mathrm{d}} \in \mathbb{C}^{1 \times M}$ and $\mathbf{B}^{\mathrm{d}} \in \mathbb{C}^{M \times N}$ represent downlink channels from the BS to the user k, the RIS to the user k and the BS to the RIS, respectively. The received signal at the user k can be written as

$$y_k = \sum_{j=1}^K \left(\mathbf{h}_k^{\mathrm{d}} + \mathbf{f}_k^{\mathrm{d}} \operatorname{diag}(\mathbf{v}) \mathbf{B}^{\mathrm{d}} \right) \mathbf{w}_j x_j + n_k$$

$$= \sum_{j=1}^K \left(\mathbf{h}_k^{\mathrm{d}} + \mathbf{v}^{\mathrm{H}} \mathbf{A}_k^{\mathrm{d}} \right) \mathbf{w}_j x_j + n_k,$$
(1)

where $\mathbf{A}_k^{\mathrm{d}} = \mathrm{diag}(\mathbf{f}_k^{\mathrm{d}})\mathbf{B}^{\mathrm{d}}$ is the cascaded channel between BS and the user k by reflection at the RIS. Denote the downlink chanel matrix as $\mathbf{H}_k^{\mathrm{d}} \triangleq [(\mathbf{h}_k^{\mathrm{d}})^{\mathrm{T}}, (\mathbf{A}_k^{\mathrm{d}})^{\mathrm{T}}]^{\mathrm{T}}$. Let $\mathbf{w}_k \in \mathbb{C}^{N \times 1}$ be the beamforming vector and $x_k \in \mathbb{C}$ be the symbols transmitted from the BS to the user k. $\mathbf{v} = [e^{jw_1}, \cdots, e^{jw_M}]^{\mathrm{H}}$ is the continuous phase-shift vector at the RIS, where $w_i \in [-\pi, \pi)$ is the phase shift of the i-th element, and $n_k \sim \mathcal{CN}(0, N_0)$ is the additive white Gaussian noise with zero mean and variance N_0 . Then, the signal to interference plus noise ratio (SINR)

at the user k can be expressed as

$$\gamma_k = \frac{\left| \mathbf{G}_k^{\mathrm{d}} \mathbf{w}_k \right|^2}{\sum_{j \neq k} \left| \mathbf{G}_k^{\mathrm{d}} \mathbf{w}_j \right|^2 + N_0},\tag{2}$$

where $\mathbf{G}_k^{\mathrm{d}} = \mathbf{h}_k^{\mathrm{d}} + \mathbf{v}^{\mathrm{H}} \mathbf{A}_k^{\mathrm{d}}$ represents the equivalent downlink channel. The sum rate of all users is then expressed as

$$R_{\text{sum}} = \sum_{k=1}^{K} \alpha_k \log(1 + \gamma_k), \tag{3}$$

where α_k is the weight. The problem in this paper can be formulated as maximizing the sum rate of all users while satisfying the transmit power and continuous phase constraints, and is given in the following

$$\max_{\mathbf{W}, \mathbf{v}} \qquad R_{\text{sum}} \tag{4}$$

s.t.
$$\sum_{k=1}^{K} \|\mathbf{w}_k\|^2 \le P \tag{4a}$$

$$|v_i| = 1, i = 1, \dots, M,$$
 (4b)

where $\mathbf{W} = [\mathbf{w}_1, \dots, \mathbf{w}_K]$ is the beamforming matrix at the BS. (4a) is the transmit power constraint and P denotes the maximum transmit power of the BS. (4b) is the continuous phase constraint at the RIS, and the discrete phase constraint will be given in Section V.

The above problem can be solved iteratively by classical methods when downlink CSI is available at the BS [41]. However, this iterative algorithm usually suffers from high complexity and slow convergence speed, so we consider a deep learning approach to solve the problem (4). In addition, channel reciprocity between uplink and downlink may not exist in the real case. Therefore, we assume that there is only uplink channel information on the BS and channel reciprocity does not hold. Suppose that there is a function $\Omega(\cdot)$ with inputs of uplink CSI and the outputs of the optimal beamforming matrix W and phase shift v that satisfies the constraints in problem (4). Then, the problem (4) can be reformulated as

$$\{\mathbf{w}_1, \cdots, \mathbf{w}_K; \mathbf{v}\} = \mathbf{\Omega}(\mathbf{H}_1^u, \cdots, \mathbf{H}_K^u), \tag{5}$$

where $\mathbf{H}_k^{\mathrm{u}} \triangleq [\mathbf{h}_k^{\mathrm{u}}, \mathbf{A}_k^{\mathrm{u}}]$ denotes the uplink channel matrix, and $\mathbf{A}_k^{\mathrm{u}} = \mathbf{B}^{\mathrm{u}} \mathrm{diag}(\mathbf{f}_k^{\mathrm{u}})$. $\mathbf{h}_k^{\mathrm{u}} \in \mathbb{C}^{N \times 1}$, $\mathbf{f}_k^{\mathrm{u}} \in \mathbb{C}^{M \times 1}$ and $\mathbf{B}^{\mathrm{u}} \in \mathbb{C}^{N \times M}$ represent uplink channels from the user k to the BS, the user k to the RIS and the RIS to the BS, respectively.

Generally, the closed-form expression for function $\Omega(\cdot)$ does not exist. Because any continuous-valued function may be approximated with a small approximation error according to the universal approximation theorem [37], the problem (4) can be transformed into a trainable problem. Suppose a network $\Omega(\cdot;\mu)$ with a trainable parameter set μ , then (5) can be approximated as follows

$$\{\mathbf{w}_1,\cdots,\mathbf{w}_K;\mathbf{v}\} = \mathbf{\Omega}(\mathbf{H}_1^u,\cdots,\mathbf{H}_K^u;\mu). \tag{6}$$

B. Uplink-Downlink Channel Reciprocity

In this subsection, we discuss the reciprocity relationship between uplink and downlink channels. Uplink and downlink channels are interrelated in wireless communication, but their reciprocity may or may not exist under different circumstances.

• Existence of the uplink and downlink channel reciprocity. When the communication system is in a relatively stable environment, the characteristics of the uplink and downlink channels may be similar, in which case there is uplink and downlink channel reciprocity [44]. This means that downlink CSI can be obtained directly from estimation of the uplink CSI. This reciprocity can be used to improve the performance of the communication system. If reciprocity is considered, the channel relationship between the users, the BS and the RIS can be expressed as

$$\mathbf{h}_k^{\mathrm{d}} = (\mathbf{h}_k^{\mathrm{u}})^{\mathrm{H}}, \mathbf{f}_k^{\mathrm{d}} = (\mathbf{f}_k^{\mathrm{u}})^{\mathrm{H}}, \mathbf{B}^{\mathrm{d}} = (\mathbf{B}^{\mathrm{u}})^{\mathrm{H}}. \tag{7}$$

• Absence of uplink and downlink channel reciprocity. The characteristics of the uplink and downlink channels are affected by a variety of factors, including the propagation environment, multipath effects, and antenna configurations. In these cases, the uplink and downlink channels may not be reciprocal. Following [42], we use a unitary matrix to describe the relationship between the uplink channel and the downlink channel. Unitary reciprocity is a special type of channel relationship that refers to the unitary transform relationship between the uplink channel matrix and the downlink channel matrix. Specifically, if there is a unitary transform relationship between channels, it can be expressed as

$$\mathbf{h}_k^{\mathrm{d}} = c_1(\mathbf{h}_k^{\mathrm{u}})^{\mathrm{H}} \mathbf{U}_1, \mathbf{f}_k^{\mathrm{d}} = c_2(\mathbf{f}_k^{\mathrm{u}})^{\mathrm{H}} \mathbf{U}_2, \mathbf{B}^{\mathrm{d}} = c_3(\mathbf{B}^{\mathrm{u}})^{\mathrm{H}} \mathbf{U}_3,$$
(8)

where c_1 , c_2 , c_3 are the randomly generated complex coefficients of the channels $\mathbf{h}_k^{\mathrm{u}}$, $\mathbf{f}_k^{\mathrm{u}}$, \mathbf{B}^{u} , and $\mathbf{U}_1 \in \mathbb{C}^{N \times N}$, $\mathbf{U}_2 \in \mathbb{C}^{M \times M}$, $\mathbf{U}_3 \in \mathbb{C}^{N \times N}$ are the unitary identity matrices of the channels $\mathbf{h}_k^{\mathrm{u}}$, $\mathbf{f}_k^{\mathrm{u}}$, \mathbf{B}^{u} , respectively.

III. DUAL-DRIVEN LEARNING APPROACH

In this section, we first review the traditional approach (i.e., the BCD algorithm with the downlink channel information) to solving problem (4). This approach provides labels for hybrid training neural networks which will be presented in sub-section B. Then, we focus on the dual-driven learning approach for joint beamforming and reflection optimization with only uplink CSI available at the BS.

A. BCD algorithm with the downlink channel information

The BCD algorithm [19] is widely used to solve joint optimization problems in RIS-based systems. The key idea is to divide the optimization variables into multiple blocks, and then update each block according to certain rules while fixing the remaining blocks to the values of the last update [45]. Our original optimization problem is non-convex and cannot be solved directly using convex optimization method, so BCD algorithm can reduce the computational complexity, especially in high-dimensional optimization problems. Specifically, the original problem (4) can be decomposed into two sub-problems, namely, the conventional beamforming design

problem, and the phase-shift optimization problem, which are given in the following

$$\max_{\mathbf{W}} \qquad R_{\text{sum}}$$
s.t.
$$\sum_{k=1}^{K} \|\mathbf{w}_k\|^2 \le P, \qquad (9)$$

$$\max_{\mathbf{v}} \qquad R_{\text{sum}}$$
s.t. $|v_i| = 1, i = 1, \dots, M.$ (10)

We first focus on the sub-problem of conventional beamforming design. Given the phase shift v, the sub-problem of optimizing W reduces to the weighted sum rate (WSR) maximization problem of a conventional multi-user MISO system, which has been widely applied, and the weighted minimum mean square error (WMMSE) algorithm [46] is a very well-known method.

Then, we focus on the sub-problem of phase optimization. Given fixed W, we can obtain optimal v through Riemannian manifold optimization method as in [19], which is a specific type of manifold optimization method [47]. Denote the direct channel and the cascade channel as follows

$$\mathbf{a}_{j,k} = \mathbf{A}_k^{\mathrm{d}} \mathbf{w}_j, \tag{11}$$

$$b_{j,k} = \mathbf{h}_{s,k}^{\mathrm{d}} \mathbf{w}_{j}, \tag{12}$$

and then the objective function can be re-written as

$$cost(x) = \sum_{k=1}^{K} \log \left(1 + \frac{|xa_{k,k} + b_{k,k}|^2}{\sum_{j \neq k} |xa_{j,k} + b_{j,k}|^2 + N_0} \right).$$
(13)

We can calculate the Riemannian gradient of this objective function as follows

$$egrad(x) = \sum_{k=1}^{K} 2\mathbf{F}_k, \tag{14}$$

$$\mathbf{F}_{k} = \frac{\sum_{j} \mathbf{a}_{j,k} b_{j,k}^{\mathrm{T}} + \sum_{j} \mathbf{a}_{j,k} \mathbf{a}_{j,k}^{\mathrm{H}} \mathbf{x}^{\mathrm{H}}}{\sum_{j} |b_{j,k} + \mathbf{x} \mathbf{a}_{j,k}|^{2} + N_{0}}$$

$$-\frac{\sum_{j \neq k} \mathbf{a}_{j,k} b_{j,k}^{\mathrm{T}} + \sum_{j \neq k} \mathbf{a}_{j,k} \mathbf{a}_{j,k}^{\mathrm{H}} \mathbf{x}^{\mathrm{H}}}{\sum_{j \neq k} |b_{j,k} + \mathbf{x} \mathbf{a}_{j,k}|^{2} + N_{0}}.$$
(15)

We set the step size to 1, and then proceed to use the step size and gradient to constantly update the current point to move to a new position on the manifold to find the point on the manifold or an approximation of the optimal value.

B. Dual-driven learning approach with uplink CSI

The BCD algorithm has two main limitations. Firstly, it suffers from a high complexity due to the nature of iterative algorithms. In particular, it contains both inner and outer iterations, where the outer iterative algorithm solves the problems (9) and (10), respectively, and the solution of each sub-problem also consists of this multi-step iteration. This practice limits its

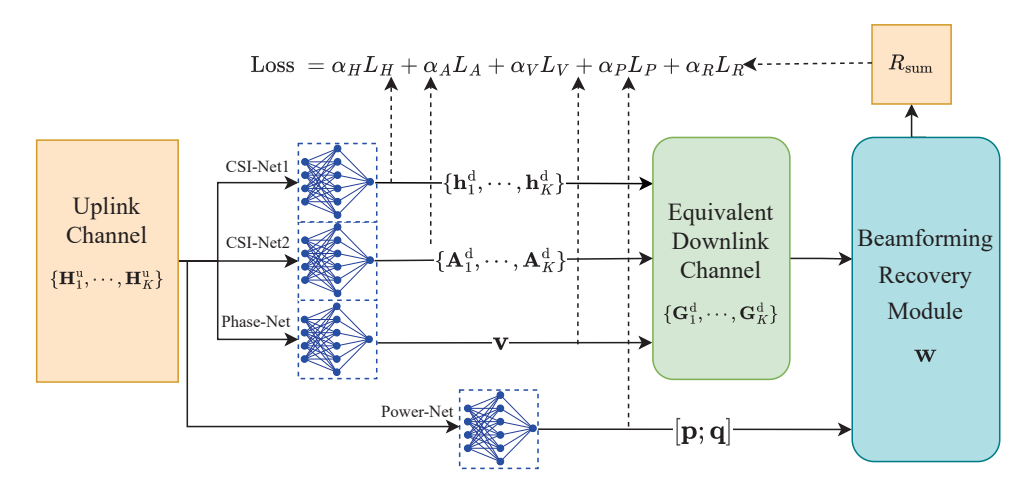


Fig. 2: Model-driven neural network framework.

application in practical systems, especially for delay-sensitive applications. Another challenge is that the BCD algorithm cannot be directly applied to the case where the BS only knows the uplink channel information. Therefore, we focus on the deep learning-based solution method which uses neural networks to learn the relationship between the input (i.e., uplink channel information) and the output (optimal solution), thus bypassing the complex iterative solution process. This method is based on the fact that a well-designed deep neural network has the ability to approximate any continuous-valued function with arbitrarily small approximation errors, as demonstrated in [43].

Optimal beamforming structure for RIS-assist MISO system

Unlike common data-driven learning, we use a model-based beamforming structure as in [41] reduce the neural network's output dimension and to improve the training efficiency and performance. It is worth noting that this structure was originally designed for multi-antenna MISO systems. It cannot be directly applied in RIS-assisted MISO systems because RIS systems include complex direct and cascade channels, as well as phase-shift vectors. However, given a fixed phase transfer vector v, the RIS system can be equivalently treated as a multiuser MISO system from a mathematical point of view. Thus, the optimal beamforming structure for RIS-assisted MISO system is given by

$$\mathbf{w}_{k} = \sqrt{p_{k}} \frac{\left(\mathbf{I}_{N} + \sum_{j=1}^{K} \frac{q_{j}}{N_{0}} (\mathbf{G}_{j}^{d})^{H} \mathbf{G}_{j}^{d}\right)^{-1} (\mathbf{G}_{k}^{d})^{H}}{\left\|\left(\mathbf{I}_{N} + \sum_{j=1}^{K} \frac{q_{j}}{N_{0}} (\mathbf{G}_{j}^{d})^{H} \mathbf{G}_{j}^{d}\right)^{-1} (\mathbf{G}_{k}^{d})^{H}\right\|}, \forall k, (16)$$

where $\mathbf{I}_N \in \mathbb{R}^{N \times N}$ denotes an identity matrix. p_k and q_k are both positive parameters satisfying $\sum_{k=1}^K p_k = \sum_{k=1}^K q_k = P$. $\mathbf{p} = [p_1, \dots, p_K]^T$ is the optimal downlink power vector, and $\mathbf{q} = [q_1, \dots, q_K]^T$ is an auxiliary vector variable that can be used to determine the beamforming direction. The power vector $[\mathbf{p}; \mathbf{q}]$ is considered as a key feature of the beamforming solution. Unlike the direct learning of the high-dimensional

beamforming matrix W, (16) enables us to learn the low-dimensional power features $[\mathbf{p}; \mathbf{q}]$. Then, the beamforming vector can be recovered from the learned power feature $[\mathbf{p}; \mathbf{q}]$ by (16). This practice reduces the output dimension of the neural network learning beamforming from 2NK to 2K, which in turn improves the training efficiency.

• The overall neural network freamwork

Based on the optimal beamforming structure (16), we propose a neural network framework to jointly learn the phase-shifts \mathbf{v} and the power feature $[\mathbf{p}; \mathbf{q}]$ that maxmizes the sum rate while adhering to the transmit power constraint and the phase shift constraint. The proposed neural network takes uplink CSI $\{\mathbf{H}_1^{\mathrm{u}}, \cdots, \mathbf{H}_K^{\mathrm{u}}\}$ as inputs and final outputs are the beamforming matrix \mathbf{W} and phase-shifts \mathbf{v} at the RIS. The overall neural network framework is depicted in Fig. 2, which consists of four modules and is described in detail below:

CSI-Net: The CSI-Net consists of CSI-Net1 and CSI-Net2, which are two fully-connected neural networks (FCNNs) used to learn the uplink-downlink relationship (i.e., the unitary transform relationship) for the direct channel and the cascade channel, respectively. The inputs of both CSI-Net1 and CSI-Net2 are uplink CSI $\{\mathbf{H}_1^{\mathrm{u}}, \cdots, \mathbf{H}_K^{\mathrm{u}}\}$. The outputs of CSI-Net1 are the predicted downlink CSI $\{\mathbf{h}_1^\mathrm{d},\cdots,\mathbf{h}_K^\mathrm{d}\}$ and the outputs of CSI-Net2 are predicted cascade CSI $\{A_1^d, \dots, A_K^d\}$. We train both networks using supervised learning methods. Since it's input is a complex matrix, we split it into real and imaginary parts to facilitate neural network training. Suppose there is a channel training dataset with T uplink-downlink CSI pairs. Denote the predicted outputs of CSI-Net1 and CSI-Net2 as $\hat{\mathbf{h}}_{k,t}^{\mathrm{d}}$ and $\hat{\mathbf{A}}_{k,t}^{\mathrm{d}}$ $(k=1,\cdots,K,t=1,\cdots,T)$, respectively, where the corresponding labels refering to the real channels are denoted as $\mathbf{h}_{k,t}^{\mathrm{d}}$ and $\mathbf{A}_{k,t}^{\mathrm{d}}$, respectively. The mean square error (MSE) is adopted as the loss functions for CSI-Net1 and CSI-Net2, which are given as follows

$$L_H = \frac{1}{2TNK} \sum_{k=1}^{K} \sum_{t=1}^{T} \|\mathbf{h}_{k,t}^{d} - \hat{\mathbf{h}}_{k,t}^{d}\|^2,$$
(17)

$$L_A = \frac{1}{2TMK} \sum_{k=1}^{K} \sum_{t=1}^{T} \|\mathbf{A}_{k,t}^{d} - \hat{\mathbf{A}}_{k,t}^{d}\|^2.$$
 (18)

Phase-Net: This module aims to learn and optimize phase-shifts \mathbf{v} at the RIS. Specifically, the neural network takes the uplink CSI $\{\mathbf{H}_1^{\mathrm{u}},\cdots,\mathbf{H}_K^{\mathrm{u}}\}$ as input and outputs the phase-shifts \mathbf{v} in a supervised learning manner. Similarly, we divide the complex vector \mathbf{v} into real and imaginary parts. Denote the predicted output of Phase-Net as $\hat{\mathbf{v}}_t$ and its label is denoted as \mathbf{v}_t . Meanwhile, the MSE-based loss function of Phase-Net is given as follows

$$L_V = \frac{1}{2TM} \sum_{t=1}^{T} \|\mathbf{v}_t - \hat{\mathbf{v}}_t\|^2.$$
 (19)

Power-Net: The Power-Net aims to learn the power feature of the beamforming solution $[\mathbf{p}; \mathbf{q}]$. We denote that the predicted outputs of Power-Net are $\hat{\mathbf{p}}_t$ and $\hat{\mathbf{q}}_t$. The \mathbf{p}_t and \mathbf{q}_t are the t-th training samples of the downlink and uplink power vectors obtained by the BCD algorithm in the power training database, respectively. Similar to the previous networks, we use a supervised learning method to train this network. Meanwhile, the loss function of Power-Net is given as follows

$$L_P = \frac{1}{2TK} \sum_{t=1}^{T} (\|\mathbf{p}_t - \hat{\mathbf{p}}_t\|^2 + \|\mathbf{q}_t - \hat{\mathbf{q}}_t\|^2).$$
 (20)

Beamforming Recovery Module: This module aims to recover the optimal beamforming. We first use the estimated direct and cascade channels and the eatimated phase-shifts to obtain the equivalent downlink CSI $\{G_1^d, \cdots, G_K^d\}$. The beamforming matrix **W** is then recovered using the power features and the equivalent downlink channel information. Note that this module does not contain any training parameters and only computes the beamforming matrix **W** via (16).

C. Hybrid training

In the training stage, the overall loss function is given as follows

Loss =
$$\alpha_H L_H + \alpha_A L_A + \alpha_V L_V + \alpha_P L_P + \alpha_R L_R$$
, (21)

where $\alpha_i, i \in \{H, A, V, P, R\}$ is the weight for each loss component. The learning of the channel matrices, phase-shift vector and power features is only an intermediate process, and our ultimate goal is to maximize sum rate of the system, so we add sum rate as an additional part of the overall loss function, i.e., $L_R = -R_{\text{sum}}$. We adopt a hybrid training method as in [31], where the downlink CSI, power features, and the phase shift vector are trained in a supervised manner, and the sum rate is trained via the unsupervised manner.

The proposed neural network model utilizes a multi-layer perceptron (MLP) architecture, with computational complexity primarily determined by the number of hidden layers and neurons. The input matrices are flattened into a one-dimensional vector before being fed into the proposed neural network framework, resulting in an input dimension of F = 2(M+1)NK. For **CSI-Net1**, we have four fully connected layers with A neurons each; for **CSI-Net2**, four

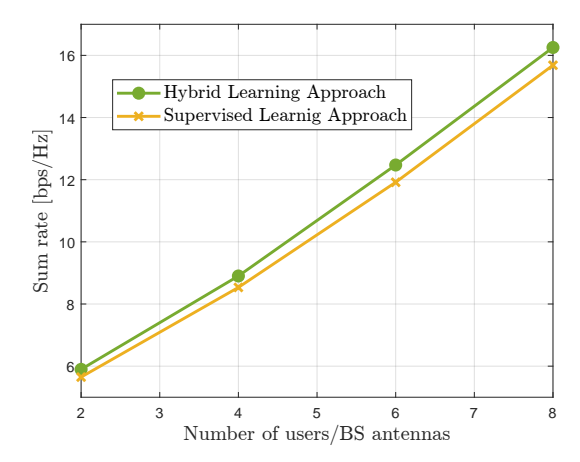


Fig. 3: Sum rate versus the number of users/BS antennas.

layers with B neurons; for **Power-Net**, four layers with C neurons; and for **Phase-Net**, four layers with D neurons. The total computational complexity of the four neural networks is approximately $O(FA+A^2+FB+B^2+FC+C^2+FD+D^2)$. The computational complexity of the beamforming matrix recovery is $O(N^3+KN^2+KMN)$. Therefore, the overall computational complexity of the proposed neural network framework is $O((FA+A^2+FB+B^2+FC+C^2+FD+D^2)+(N^3+KN^2+KMN))$.

Fig. 3 shows the rate performance comparison between the hybrid training method and the supervised training method which has a similar loss function as in (21) but does not include rate loss. The transmit power of the downlink channel is 30 dBm, and the number of passive reflect elements is 32. The performance of hybrid learning achieves improved sum rate performance than that of the supervised learning method. For example, when the number of users and transmit antennas at the BS is 6, the sum rate of the supervised learning method is 11.9 bps/Hz, about 5% lower than that of the hybrid learning method. Fig. 4 depicts the respective loss training curves of the sub-networks with different number of transmit antennas, and we can observe that after training for multiple epochs, the loss of each sub-network converges stably. Fig. 5 depicts the total loss training curve of the overall neural network under different hyper-parameters. The performance of the total loss is affected by the hyper-parameters. This means that we need to fine-tune the hyper-parameters of the neural network to achieve better performance.

D. Discrete Phase Shifts

While the aforementioned studies focused on the study of continuous phases of reflective elements, in this subsection, we will extend the problem of optimizing RIS-assisted MISO systems under continuous phase constraints to practical discrete phase constraints [20], [21]. For practical implementation, we consider that the phase shift of each element of the RIS can only take a finite number of discrete values. Let b denote the number of bits used to represent the phase shift level L, where $L=2^b$. For simplicity, we assume that these phase shift values are obtained by uniformly quantizing the

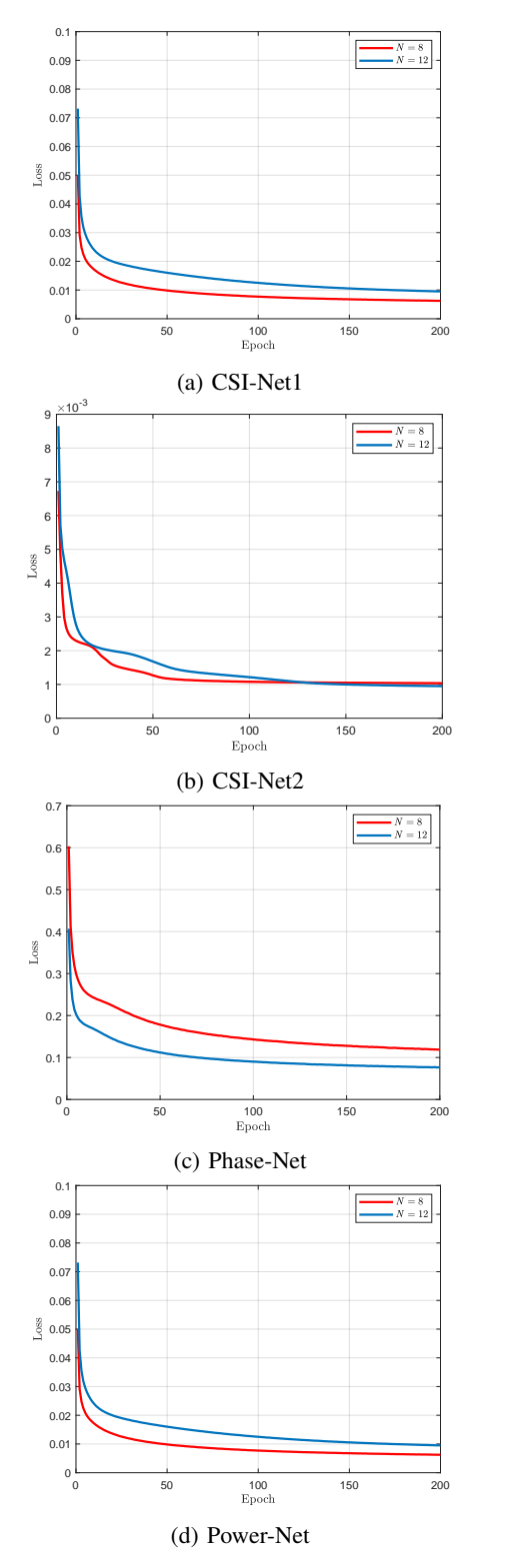


Fig. 4: Loss function value versus training epochs.

interval $[-\pi, \pi)$. Thus, the set of discrete phase shifts at each reflective element is given by

$$\mathcal{F} = \{-\pi, -\pi + \Delta\theta, -\pi + 2\Delta\theta, \dots, -\pi + (L-1)\Delta\theta\},\tag{22}$$

where $\Delta\theta = 2\pi/L$. $\mathbf{v} = [e^{j\theta_1}, \cdots, e^{j\theta_M}]^H$ is the discrete phase-shift vector at the RIS, where θ_i is the phase shift of

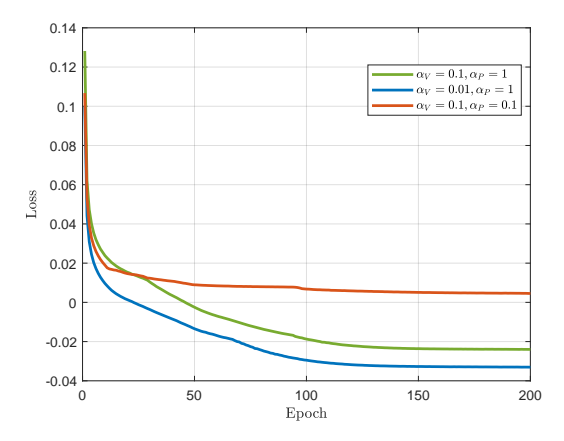


Fig. 5: The final loss function value versus training epochs (N = 8).

the i-th element. Then the original optimization problem (4) can be reformulated as follows

$$\max_{\mathbf{W},\mathbf{v}} \qquad R_{\text{sum}} \tag{23}$$

s.t.
$$\sum_{k=1}^{K} \|\mathbf{w}_k\|^2 \le P$$
 (23a)

$$\theta_i \in \mathcal{F}, i = 1, \dots, M.$$
 (23b)

The optimization problem in (23) is non-convex due to the coupling of \mathbf{W} and \mathbf{v} . Furthermore, the constraints in (23b) restrict θ_i to be discrete. Following [20], we employ an efficient successive refinement algorithm to solve this optimization problem by extending the channel gain expression. Let $\mathbf{C} = \mathbf{A}_k^{\mathrm{d}}(\mathbf{A}_k^{\mathrm{d}})^{\mathrm{H}}$ and $\mathbf{b} = \mathbf{A}_k^{\mathrm{d}}(\mathbf{h}_k^{\mathrm{d}})^{\mathrm{H}}$. The channel gain is given by

$$\|\mathbf{h}_{k}^{d} + \mathbf{f}_{k}^{d} \operatorname{diag}(\mathbf{v}) \mathbf{B}^{d}\|^{2} = \mathbf{v}^{H} \mathbf{C} \mathbf{v} + 2Re\{\mathbf{v}^{H} \mathbf{b}\} + \|\mathbf{h}_{k}^{d}\|^{2}.$$
(24)

Assuming that all other reflecting elements $(\theta_{\xi}, \forall \xi \neq m, m \in M)$ are fixed, and focusing only on a single reflecting element θ_m , the channel gain can be written as [20]

$$2Re\{e^{j\theta_m}\zeta_m\} + \tau_m,\tag{25}$$

where $\zeta_m = \sum_{\xi \neq m} C_{m\xi} e^{-j\theta_\xi} + b_m \triangleq |\zeta_m| e^{-j\varphi_m}$ and $\tau_m = \sum_{\xi \neq m} \sum_{i \neq m} C_{\xi i} e^{j(\theta_\xi - \theta_i)} + 2Re\{\sum_{\xi \neq m} e^{j\theta_\xi} b_\xi\} + C_{mm} + \|b\|^2$, where $C_{\xi i}$ and b_ξ represent the individual elements of C and b, respectively. Let ϵ denotes the stopping threshold for convergence. Then the successive refinement algorithm is summarized in Algorithm 1

Algorithm 1 Successive Refinement algorithm [21]

```
1: initialize \mathbf{v} = \mathbf{v}^{(0)}

2: set \lambda = 0

3: R^{(0)} = R_{\mathrm{sum}}^{(0)}

4: while |R^{(\lambda)} - R^{(\lambda-1)}| > \epsilon do

5: for m = 1 to M do

6: \theta_m^* = \arg\min_{\theta \in \mathcal{F}} |\theta - \varphi_m|

7: \lambda = \lambda + 1

8: R^{(\lambda)} = R_{\mathrm{sum}}^{(\lambda)}

9: end for

10: end while
```

However, this successive refinement algorithm achieves the optimal or near-optimal solution by stepwise optimization, and thus converges slowly. Therefore, we consider the proposed dual-driven learning approach to solve the problem (23). Specifically, we first utilized the model framework in Fig. 2 to train four sub-networks for obtaining the predicted values of downlink direct channel, downlink cascade channel, reflection phase shifts and power features, respectively. Different from the above approach, we process the continuous phase shifts obtained from Phase-Net. After prediction, we map the continuous phase values to discrete phase values to obtain the final prediction. For specific implementation, we calculate the distance between each continuous output value and discrete phase value based on the shortest distance principle, and select the closest discrete phase value as the mapping target. Finally, we learn the downlink beamforming matrix based on the proposed optimal beamforming structure to maximize the system sum rate.

IV. NUMERICAL RESULTS

In this section, we evaluate the performance of the proposed approach. Unless otherwise specified, the RIS-assisted multiuser MISO system includes a BS with N=6 antennas, a RIS with M=32 passive reflective elements, and K=3 single antenna users. Weight $\alpha_k=1, \forall k$. The (x,y,z) coordinates (in meters) of the RIS and the BS positions are (0,0,0) and (100,-100,0), respectively. Users are uniformly distributed in a rectangular region $[5,30]\times[-30,30]$ in the (x,y) plane at z=-20. The total transmit power of the BS is 30 dBm and the noise power is -120 dBm.

We use Rayleigh fading to model the direct channel from multiusers to the BS as follows

$$\mathbf{h}_k^{\mathbf{u}} = L_{1,k} \tilde{\mathbf{h}}_k^{\mathbf{u}},\tag{26}$$

where $\tilde{\mathbf{h}}_k^{\mathrm{u}}$ denotes Rayleigh fading and follows $\mathcal{CN}(\mathbf{0},\mathbf{I})$. $L_{1,k}$ denotes the path loss (in dB) of the direct channel from the user k to the BS as $32.6+36.7\log(d_k^{\mathrm{UB}})$, where d_k^{UB} (in meter) is the distance between the user k and the BS [19].

We use Rician fading to model the channels \mathbf{B}^{u} and $\mathbf{f}_k^{\mathrm{u}}$ as follows

$$\mathbf{B}^{\mathrm{u}} = L_{2}(\sqrt{\frac{\varepsilon}{1+\varepsilon}}\tilde{\mathbf{B}}^{\mathrm{LOS}} + \sqrt{\frac{1}{1+\varepsilon}}\tilde{\mathbf{B}}^{\mathrm{NLOS}}), \quad (27)$$

$$\mathbf{f}_{k}^{\mathrm{u}} = L_{3,k} \left(\sqrt{\frac{\varepsilon}{1+\varepsilon}} \tilde{\mathbf{f}}_{k}^{\mathrm{LOS}} + \sqrt{\frac{1}{1+\varepsilon}} \tilde{\mathbf{f}}_{k}^{\mathrm{NLOS}} \right), \tag{28}$$

where $\varepsilon=10$ is the Rician factor, L_2 (in dB) stands for the path loss from the RIS to the BS as $30+22\log(d^{\mathrm{IB}})$, and $L_{3,k}$ (in dB) denotes the path loss from the user k to the RIS as $30+22\log(d_k^{\mathrm{UI}})$. d^{IB} and d_k^{UI} (in meters) are the distances between the RIS and the BS, and between the user k and the RIS, respectively [18]. The superscript LOS and NLOS represent the line-of-sight part and the non-line-of-sight part of the channel, respectively. The NLOS parts are modeled as standard Gaussian distribution, i.e., $[\tilde{\mathbf{B}}^{\mathrm{NLOS}}]_{ij} \sim \mathcal{CN}(0,1)$ and $[\tilde{\mathbf{f}}_k^{\mathrm{NLOS}}]_i \sim \mathcal{CN}(0,1)$.

The LOS parts are the function of the BS/RIS/user k locations. Denote the superscripts azi and ele as the azimuth and elevation angles, respectively. Similar to [48], $\theta_1^{\rm azi}$, $\theta_1^{\rm ele}$ denote the azimuth and elevation angles of arrival (AoA) to the BS, respectively. $\phi_2^{\rm azi}$, $\phi_2^{\rm ele}$ are the azimuth and elevation angles of departure (AoD) from the RIS to the BS, respectively. $\varphi_{3,k}^{\rm azi}$, $\varphi_{3,k}^{\rm ele}$ are the azimuth and elevation angles of arrival from the user k to the RIS, respectively. The steering vectors of the BS can be given by

$$\mathbf{a}_{\text{BS}}(\theta_1^{\text{azi}}, \theta_1^{\text{ele}}) = [1, \cdots, e^{j\pi(M-1)\cos(\theta_1^{\text{azi}})\cos(\theta_1^{\text{ele}})}].$$
 (29)

Then the LOS part of $\tilde{\mathbf{B}}$ can be written as [29]

$$\tilde{\mathbf{B}}^{LOS} = \mathbf{a}_{BS}(\theta_1^{azi}, \theta_1^{ele}) \mathbf{a}_{RIS}(\phi_2^{azi}, \phi_2^{ele})^{H}.$$
 (30)

Similarly, the n-th element of the RIS steering vector $\mathbf{a}_{\mathrm{RIS}}(\varphi_{3,k}^{\mathrm{azi}},\varphi_{3,k}^{\mathrm{ele}})$ can be given by

$$\left[\mathbf{a}_{\text{RIS}}(\varphi_{3,k}^{\text{azi}}, \varphi_{3,k}^{\text{ele}})\right]_{n} = e^{j\pi\left\{i_{1}(n)\sin\left(\varphi_{3,k}^{\text{azi}}\right)\cos\left(\varphi_{3,k}^{\text{ele}}\right)+i_{2}(n)\sin\left(\varphi_{3,k}^{\text{ele}}\right)\right\}},$$
(31)

where $i_1(n) = \text{mod}(n-1,10)$ and $i_2(n) = \lfloor (n-1)/10 \rfloor$. Then the LOS part of $\tilde{\mathbf{f}}_k$ can be given as

$$\tilde{\mathbf{f}}_{k}^{\text{LOS}} = \mathbf{a}_{\text{RIS}}(\varphi_{3.k}^{\text{azi}}, \varphi_{3.k}^{\text{ele}}). \tag{32}$$

Let (x_k, y_k, z_k) , $(x^{\rm RIS}, y^{\rm RIS}, z^{\rm RIS})$ and $(x^{\rm BS}, y^{\rm BS}, z^{\rm BS})$ denote the location of the user k, the RIS and the BS, respectively. Then we have

$$\cos(\theta_1^{\text{azi}})\cos(\theta_1^{\text{ele}}) = \frac{x^{\text{RIS}} - x^{\text{BS}}}{d^{\text{IB}}},\tag{33}$$

$$\sin\left(\phi_2^{\text{azi}}\right)\cos(\phi_2^{\text{ele}}) = \frac{y^{\text{BS}} - y^{\text{RIS}}}{d^{\text{IB}}},\tag{34}$$

$$\sin(\phi_2^{\text{ele}}) = \frac{z^{\text{BS}} - z^{\text{RIS}}}{d^{\text{IB}}},\tag{35}$$

$$\sin\left(\varphi_{3,k}^{\text{azi}}\right)\cos(\varphi_{3,k}^{\text{ele}}) = \frac{y_k - y^{\text{RIS}}}{d_k^{\text{UI}}},\tag{36}$$

$$\sin\left(\varphi_{3,k}^{\text{ele}}\right) = \frac{z_k - z^{\text{RIS}}}{d_k^{\text{UI}}}.$$
 (37)

A. Continuous Phase-shifts with Non-reciprocal Channel

We implement the proposed network using the deep learning library TensorFlow [49] which is trained through 10^5 training samples and 10^3 test samples. We use the Adam optimizer [50] with an initial learning rate of 10^{-3} . The structure and hyper-parameters of the proposed neural network are shown in Table I and Table II.

TABLE I: Neural Network Hyperparameter

	CSI-Net1	CSI-Net2	Phase-Net	Power-Net	
Number of hidden layers	4	4	5	2	
Hidden layers activation	relu	relu	relu	relu	
Output layer activation	tanh	tanh	tanh	softmax	
Batchsize	256	256	256	256	

TABLE II: Number of Neurons

CSI-Net1	{1024,512,256,128}
CSI-Net2	{1024,512,256,128}
Phase-Net	{1024,1024,512,256,128}
Power-Net	{1024,512,128}

We compare the proposed approach with the following benchmarks.

- *Perfect CSI with BCD*: This approach first assumes that the perfect downlink CSI are known at the BS, and we use the BCD algorithm [19] to solve the sum rate maximization problem (4), and resulting sum rate performance is used as the upper bound for comparison.
- **ZF-based learning apporach**: This approach first learns the downlink CSI, power features and phase-shift vector through supervised training of the neural networks, and then uses the learned information to construct the beamforming via zero-forcing (ZF) structure [51].
- *MRT-based learning apporach*: This approach is also similar with the proposed solution except that we use the maximum ratio transmission (MRT) beamforming structure [52] rather than the structure in (16).

Table III depicts the comparison between the Perfect CSI with BCD method and the proposed solution in terms of execution time for 1000 samples with different number of RIS elements (i.e., M). The execution time of both methods increases with the increase of M, and the execution time of our method is significantly smaller than that of the traditional BCD method. For example, when M=32, the proposed method takes about 1.43 s to complete 1000 samples, which is about 3 percent of the BCD algorithm execution time.

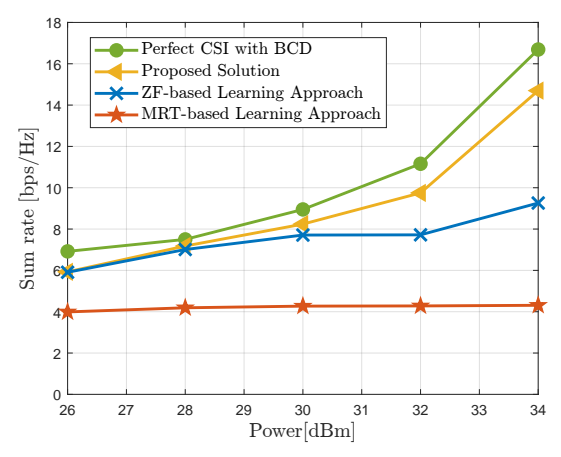


Fig. 6: Sum rate versus the transmit power.

Fig. 6 shows that the sum rate performance of four methods increases with the increasing transmit power, because the higher the transmit power, the stronger the signal received by

the wireless terminal and the better the beamforming effect. The sum rate of the proposed approach is close to that of the BCD algorithm with perfect CSI, and it outperforms that of ZF and MRT beamforming based learning methods. For example, when the transmit power is equal to 30 dBm, the sum rate of the proposed solution achieves around 8.24 bps/Hz, about 6.87% and 92.97% higher than that of ZF-based and MRT-based learning approaches respectively. The reason lies in that ZF beamforming only focuses on interference cancellation, and ignores the negative effect arising from noise, thus suitable for high signal to noise ratio (SNR) scenarios, while MRT adapts to low SNR scenarios because it focuses on the noise minimization. In contrast, the proposed method adopts the optimal beamforming structure (16) considering both interference cancellation and noise reduction, so it obtains improved rate performance. The MRT beamforming solution has the worst sum rate performance which remains almost unchanged. This is because the beamforming matrix (16) of the RIS system is affected by the direct channel, the cascaded channel, and the phase shift vectors, whereas the MRT method with only simpler beamforming structures (i.e., conjugate transposition of the downlink channel) does not allow for any further improvement in the rate performance, even for larger transmit power. This imply that MRT is unsuitable to be the beamforming method for RIS-assisted multiuser MISO system.

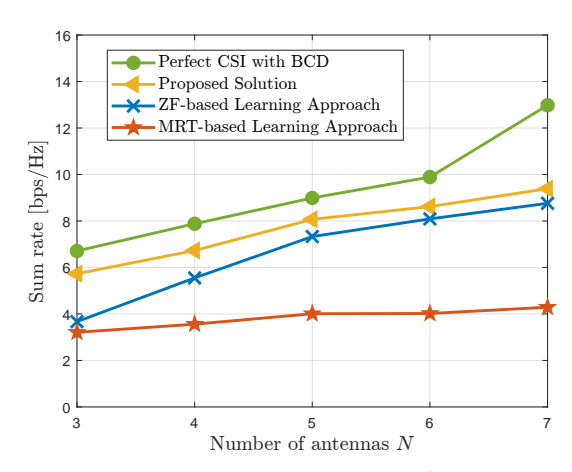


Fig. 7: Sum rate versus the number of BS antennas at $[3, \dots, 7]$.

Fig. 7 shows the sum rate versus the number of BS's antennas N. The sum rates of the BCD with the perfect CSI method, the proposed approach and the ZF-based method have improved with the increasing number of transmit antennas at the BS (i.e., N), because more antennas increases the diversity gain in multi-antenna system. Once again, the proposed method achieves higher rate performance compared with ZF-and MRT-based methods due to the efficient beamforming structure. For instance, when N equals 5, the sum rate of the proposed scheme reaches about 8.07 bps/Hz, about 10.09% and 101.25% higher than that of the ZF-based and MRT-based learning methods, respectively.

In Fig. 8, as the number of antennas increases from 8 to 12, the sum rates of the perfect CSI method, our proposed method,

TABLE III: Comparison of execution time for different methods.

Number of RIS Elements Method	8	16	32	48	64
Perfect CSI with BCD (s)		38.64	42.46	64.25	168.65
Proposed Solution (s)		1.17	1.43	1.55	1.66

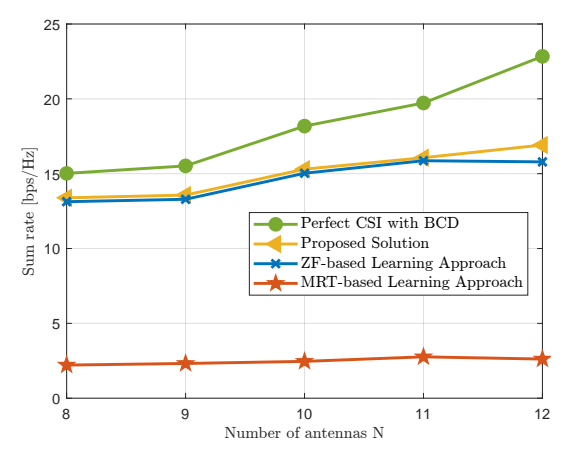


Fig. 8: Sum rate versus the number of BS antennas at $[8, \cdots, 12]$.

and the ZF and MRT-based methods all show improvement. In comparison, the rate of the ZF-based method increases from 13.12 bps/Hz to 15.77 bps/Hz, which is close to our method but slightly lower. The sum rate of the MRT-based method is the lowest, with a small increase from 2.23 bps/Hz to 2.62 bps/Hz. Overall, our proposed method continues to outperform the ZF and MRT-based methods as the number of antennas increases.

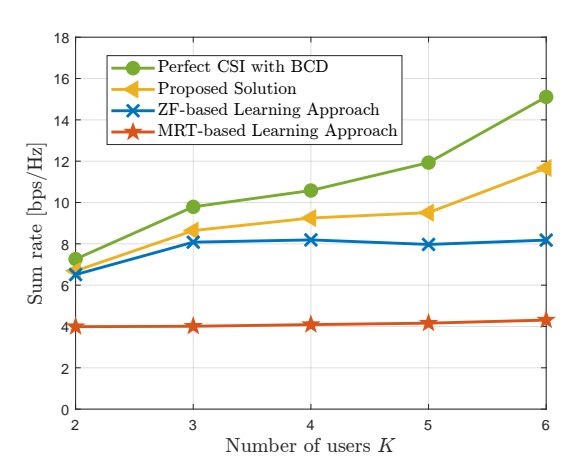


Fig. 9: Sum rate versus the number of users.

Fig. 9 shows the sum rate versus the number of users K. The sum rate increases with the increasing number of users, because the multiplexing gain of multi-antenna and RIS. Meanwhile, the proposed approach still has improved sum rate compared with ZF-based and MRT-based methods. For example, when K is equal to 4, the sum rate of the proposed solution achieves 9.25 bps/Hz, about 12.94% and 126.16% higher than that of ZF-based and MRT-based methods, respectively.

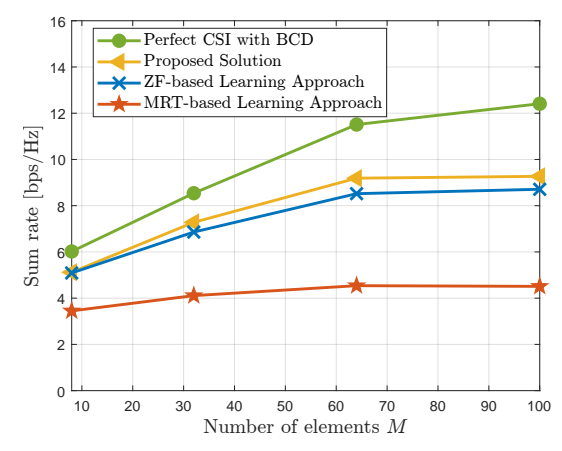


Fig. 10: Sum rate versus the number of elements.

Fig. 10 shows the sum rate versus the number of passive reflect elements M at the RIS. The sum rate increases with the increasing the number of RIS elements, because more reflective elements make the RIS more flexible, allowing it to precisely control the direction of the reflected signals and extend the communication range. Likewise, the sum rate of the proposed approach outperforms other benchmarks. For instance, when M is equal to 100, the sum rate of the proposed method achieves 9.19 bps/Hz, about 7.86% and 102.42% higher than that of ZF-based and MRT-based approaches, respectively.

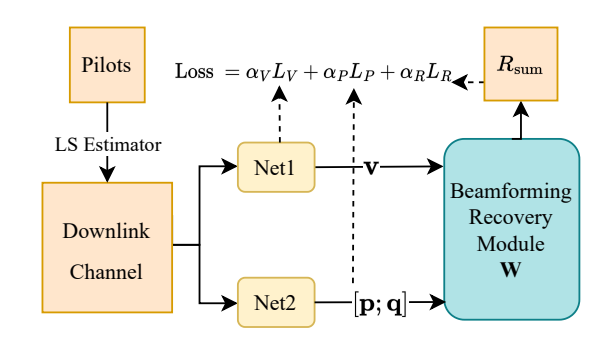


Fig. 11: Simplified neural network framework.

B. Continuous Phase-shifts with Reciprocal Channel

Now, we will compare our proposed method with the state-of-the-art method in [29], which adopts a GNN with the pilot signal as the inputs to direct learn the beamforming matrix \mathbf{W} and the phase shift vector \mathbf{v} without the aid of beamforming

structure. However, since this methods assumes the availability of channel reciprocity, it is hard to compare with our method directly. To address this problem, we also consider channel reciprocity, and adopt Least Squares (LS) [53] to estimate the downlink CSI, which is used as the input of the overall neural network. Because the channel reciprocity is hold, **CSI-Net** is not necessary, and we provide a simpler network framework where two FCNNs learn the power feature $[\mathbf{p}; \mathbf{q}]$ and the phase shift vector \mathbf{v} , followed by which we recover beamforming matrix via (16) and then calculate the sum rate, as shown in Fig. 11.

Next, we will briefly introduce the pilot generation and the LS channel estimation method. We divide the total training slots F into λ sub-frames, each with $F_0=K$ symbols, and thus $F=\lambda F_0$. Let $\mathbf{v}(x)$ be the phase-shift at the RIS in the sub-frame x. Users simultaneously send pilot sequences $\mathbf{s}_k=[s_k(1),...,s_k(F_0)]$ $(k=1,\cdots,K)$ to the BS, which is repeated in the λ sub-frames. Then, the received pilots $\mathbf{Y}(x)$ at the BS in sub-frame x can be given as

$$\mathbf{Y}(x) = \sum_{k=1}^{K} (\mathbf{h}_k^{\mathrm{u}} + \mathbf{A}_k^{\mathrm{u}} \mathbf{v}(x)) \mathbf{s}_k + \mathbf{N}(x), x = 1, ..., \lambda, \quad (38)$$

where $\mathbf{N}(x)$ is the noise matrix with each column independently distributed as $\mathcal{CN}(\mathbf{0}, \sigma_n^2 \mathbf{I})$. We use an orthogonal pilot transmission strategy, i.e., $\mathbf{s}_{k_i} \mathbf{s}_{k_i}^{\mathrm{H}} = F_0 P_u$, where P_u is the uplink pilot transmission power, and $\mathbf{s}_{k_1} \mathbf{s}_{k_2}^{\mathrm{H}} = 0$ when $k_1 \neq k_2$. Then, the received pilot of the k-th user in subframe x can be represented as [54]

$$\mathbf{y}_{k}(x) = \frac{1}{F_{0}} \mathbf{Y}(x) \mathbf{s}_{k}^{H} = \mathbf{h}_{k}^{u} + \mathbf{A}_{k}^{u} \mathbf{v}(x) + \mathbf{n}(x)$$

$$\triangleq \mathbf{H}_{k}^{u} \mathbf{e}(x) + \mathbf{n}(x),$$
(39)

where $\mathbf{n}(x) = \frac{1}{F_0} \mathbf{N}(x) \mathbf{s}_k^{\mathrm{H}}$ is the equivalent noise. The combined phase-shifts is defined as $\mathbf{e}(x) \triangleq \left[1, \mathbf{v}(x)^{\mathrm{H}}\right]^{\mathrm{H}}$. The received pilots matrix $\hat{\mathbf{Y}}_k = \left[\mathbf{y}_k(1), \dots, \mathbf{y}_k(\lambda)\right]$ can be represented as

$$\hat{\mathbf{Y}}_k = \mathbf{H}_k^{\mathrm{u}} \mathbf{E} + \mathbf{N},\tag{40}$$

where
$$\mathbf{E} = [\mathbf{e}(1), \dots, \mathbf{e}(\lambda)]$$
 and $\mathbf{N} = [\mathbf{n}(1), \dots, \mathbf{n}(\lambda)]$.

Then, we use the LS method to estimate the downlink channel matrix \mathbf{H}_k^d , which considers the existence of reciprocity between the uplink and downlink channels, i.e., the downlink channel matrix is the conjugate transpose of the uplink channel.

As shown in Fig. 11, we use downlink CSI $[\mathbf{H}_1^d, \cdots, \mathbf{H}_K^d]$ as the input of the neural networks to learn the power feature $[\mathbf{p}; \mathbf{q}]$ and the phase-shift vector \mathbf{v} . We compare the proposed solution with the following benchmarks.

- **GNN-based learning apporach** [29]: This approach uses a GNN to map the received pilot signals to the beamformer at the BS and the phase shifter at the RIS.
- LS channel estimation with BCD: This approach first estimates CSI using the LS estimator, and then solves sum rate maximization problem with the BCD algorithm [19].

Fig. 12 shows the sum rate versus the number of users K. The sum rate of our proposed method is superior to the

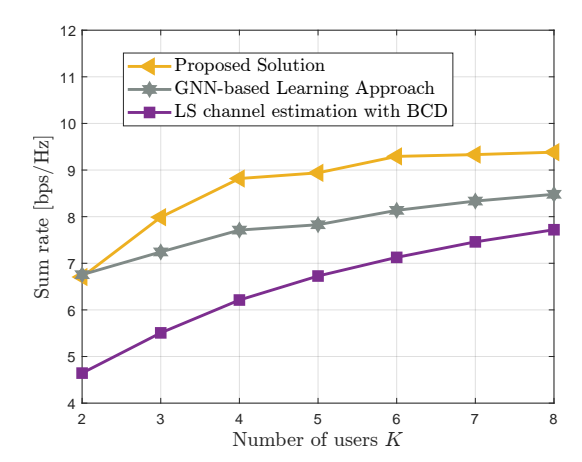


Fig. 12: Sum rate versus the number of users.

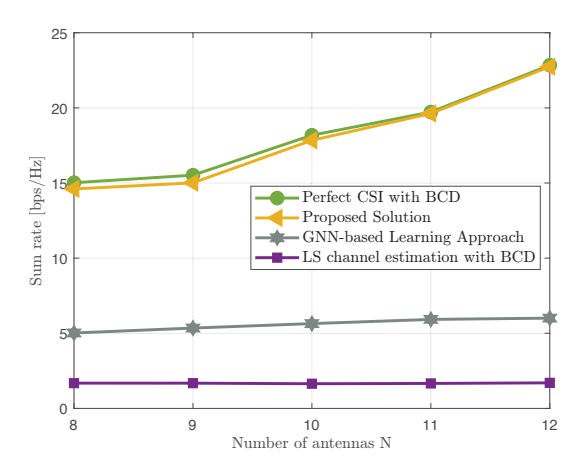


Fig. 13: Sum rate versus the number of BS antennas.

GNN-based learning approach. For instance, when K equals 4, the rate of our method achieves 8.82 bps/Hz, which is about 14.41% higher than that of GNN-based method. This is due to the fact that GNN-based direct learns the beamforming vector instead of power feature in a data driven manner, and has a larger output dimension of the neural network, thus deteriorating the training efficiency and accuracy. In contrast, our proposed method takes the advantage of optimal beamforming structure, and achieves better performance, implying that purely data-driven is insufficient, and the superior performance of our proposed data and model driven approach. In addition, the GNN-based learning method achieves a better rate performance than LS channel estimation based BCD method, and the reason is given in the following. LS channel estimation with BCD actually can be viewed as a two step approach, namely, estimating the channel and then optimizing the beamforming and the phase shift. This practice is not the rate performance oriented, and thus achieves lower rate performance. In contrast, the GNN-based learning approach joint learns the channel estimation and optimization design which focuses on the final target of maximizing the sum rate performance without pursuiting the high accuracy of channel estimation.

Fig. 13 shows the relationship between the number of antennas and the sum rate. The sum rate performance achieved

by our proposed method close to the perfect CSI with BCD and significantly outperforms the GNN-based and LS-based methods. As the number of antennas increases from 8 to 12, the performance upper bound rises from 15.02 bps/Hz to 22.84 bps/Hz, while our proposed method similarly improves from 14.61 bps/Hz to 22.75 bps/Hz, demonstrating high efficiency. In contrast, the GNN-based method grows slowly, with the sum rate only increasing from 5.02 bps/Hz to 6.01 bps/Hz, while the LS-based method shows the lowest sum rate and remains almost flat. Overall, our method significantly outperforms the GNN-based and LS-based methods, achieving performance close to the theoretical optimum.

C. Discrete Phase-shifts with Non-reciprocal Channel

In order to verify that our proposed dual-driven approach also applies to the discrete phase shifts, we compare the proposed solution with the following benchmarks.

- Perfect CSI with Successive Refinement algorithm: This approach assumes that the perfect downlink CSI are known at the BS, and uses the successive refinement algorithm [20] to solve problem (23).
- **ZF-based learning apporach**, **b=2**: This approach first uses the neural networks to learn the feature information. Then, the continuous phase is quantized into discrete values by setting b = 2, and then the beamforming is constructed by zero-forcing (ZF) structure [51]. Similarly for b = 1.

In Fig. 14, we compare the sum rate performance for different quantized phase shifts. Taking the successive refinement algorithm with perfect CSI as an upper bound, it can be found that the sum rate of the proposed discrete phase-shift method is close to the upper performance bound, and outperforms the ZF-based learning approach. In addition, we can find that the performance of the system is significantly improved when the discrete phase shift levels increasing from 1 bit to 2 bits. For instance, when the transmit power is 30 dBm, the sum rate of the proposed method achieves 6.54 bps/Hz with 1 bit discrete phase shift, while it achieves 7.97 bps/Hz with 2 bits. This is because the increased phase resolution allows the system to more accurately control the phase of the electromagnetic wave, resulting in more accurate beamforming and thus improved system performance.

D. Performance for Maximizing Minimum Rate

In practical wireless communication systems, the summation rate objective does not provide fairness among users. In this section, we consider the problem of maximizing the minimum user rate, i.e., the max-min problem, formulated as follows

$$\max_{\mathbf{W},\mathbf{v}} \quad \min_{k} R_k \tag{41}$$

$$\max_{\mathbf{W}, \mathbf{v}} \quad \min_{k} R_{k}$$
s.t.
$$\sum_{k=1}^{K} \|\mathbf{w}_{k}\|^{2} \leq P$$
(41a)

$$|v_i| = 1, \quad i = 1, \dots, M$$
 (41b)

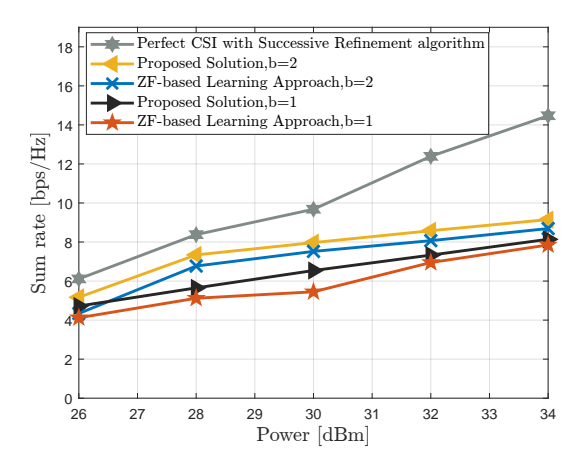


Fig. 14: Sum rate versus the transmit power for different quantized phase shifts.

For the max-min problem, we use the same neural network architecture as for the optimization problem (4), while we use the traditional BCD algorithm to provide labels for the hybrid trained neural network. The difference is that here it is based on the WMMSE algorithm to continuously and iteratively update the beamforming vectors to increase the minimum user rate, with the goal of maximizing the minimum rate by increasing the rate of the weakest user in the system as much as possible.

We employed the same neural network architecture and parameter settings as those used for the sum rate problem to address the max-min optimization problem, conducting simulation analyses in multi-antenna scenarios. Fig. 15 indicates that under ideal channel conditions, system performance significantly improves as the number of antennas increases, with the maximum user rate reaching 4.87 bps/Hz in the 10-antenna configuration. The GNN-based method exhibited relatively poor performance across all antenna configurations, achieving a maximum rate of only 0.88 bps/Hz in the 10antenna setup, highlighting its limitations in complex environments. In contrast, our proposed algorithm demonstrated significantly better performance on the max-min problem, increasing the maximum rate from 0.71 bps/Hz to 4.63 bps/Hz in the case of three users, especially achieving 3.03 bps/Hz in the nine-antenna configuration; for four users, the maximum rate improved from 1.95 bps/Hz to 3.65 bps/Hz. This indicates that our algorithm effectively enhances system performance while ensuring user fairness.

V. Conclusion

In this paper, for a RIS-assisted multi-user MISO system, we propose an optimization algorithm that directly optimizes the beamforming matrix and continuous or discrete phases shifts to maximize the sum rate of the system, provided that only the uplink channel information is known and there is no reciprocity between the uplink and downlink channels. We introduce a dual-driven approach to learn the required power features and phase-shift vector using the uplink CSI as input to the neural network, and use the structure of the optimal beamforming solution to facilitate efficient neural network

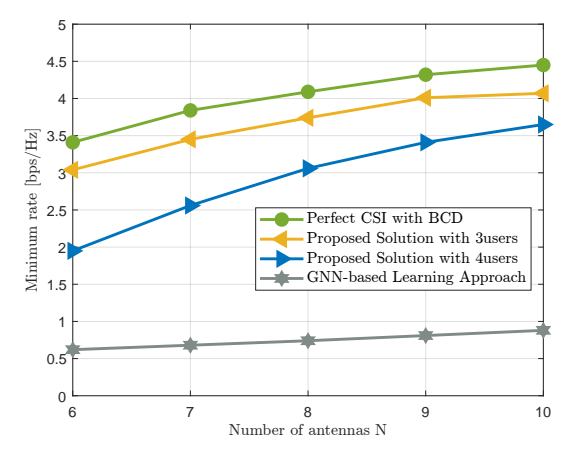


Fig. 15: Minimum rate versus the number of BS antennas.

design. Numerical results show that the proposed solution can approach the upper limit of the achieved performance for both continuous and discrete phase shifts, and achieve higher sum rate than the benchmarks. Simulation results demonstrate the importance of the dual-driven approach in downlink beamforming optimization.

REFERENCES

- S. Gong et al., "Towards smart wireless communications via intelligent reflecting surfaces: A contemporary survey," *IEEE Commun. Surveys Tuts.*, vol. 22, no. 4, pp. 2283-2314, 2020.
- [2] E. Basar, M. Di Renzo, J. De Rosny, M. Debbah, M. -S. Alouini and R. Zhang, "Wireless Communications Through Reconfigurable Intelligent Surfaces," *IEEE Access*, vol. 7, pp. 116753-116773, 2019.
- [3] C. Huang, A. Zappone, G. C. Alexandropoulos, M. Debbah and C. Yuen, "Reconfigurable Intelligent Surfaces for Energy Efficiency in Wireless Communication," *IEEE Trans. Wireless Commun.*, vol. 18, no. 8, pp. 4157-4170, Aug. 2019.
- [4] D. Li, "Bound Analysis of Number Configuration for Reflecting Elements in IRS-Assisted D2D Communications," *IEEE Wireless Commun. Lett.*, vol. 11, no. 10, pp. 2220-2224, Oct. 2022.
- [5] J. Cheng, C. Shen, Z. Chen and N. Pappas, "Robust Beamforming Design for IRS-Aided URLLC in D2D Networks," *IEEE Trans. Wireless Commun.*, vol. 70, no. 9, pp. 6035-6049, Sept. 2022.
- [6] H. Pang, F. Ji, M. Wen, S. Wang, L. Xu and Y. -C. Wu, "Interference Exploitation in IRS-Aided Heterogeneous Networks: Joint Symbol Level Precoding and Reflecting Design," *IEEE Trans. Wireless Commun.*, vol. 23, no. 6, pp. 6467-6481, June 2024.
- [7] N. Li, M. Li, Y. Liu, C. Yuan and X. Tao, "Intelligent Reflecting Surface Assisted NOMA With Heterogeneous Internal Secrecy Requirements," *IEEE Wireless Commun. Lett.*, vol. 10, no. 5, pp. 1103-1107, May 2021.
- [8] Y. Liu, F. Han and S. Zhao, "Flexible and Reliable Multiuser SWIPT IoT Network Enhanced by UAV-Mounted Intelligent Reflecting Surface," *IEEE Trans. Reliab.*, vol. 71, no. 2, pp. 1092-1103, June 2022.
- [9] J. Tang, Z. Peng, D. K. C. So, X. Zhang, K. -K. Wong and J. A. Chambers, "Energy Efficiency Optimization for a Multiuser IRS-Aided MISO System With SWIPT," *IEEE Trans. Wireless Commun.*, vol. 71, no. 10, pp. 5950-5962, Oct. 2023.
- [10] T. Shafique, H. Tabassum and E. Hossain, "Optimization of Wireless Relaying With Flexible UAV-Borne Reflecting Surfaces," *IEEE Trans. Wireless Commun.*, vol. 69, no. 1, pp. 309-325, Jan. 2021.
- [11] Y. Su, X. Pang, S. Chen, X. Jiang, N. Zhao and F. R. Yu, "Spectrum and Energy Efficiency Optimization in IRS-Assisted UAV Networks," *IEEE Trans. Wireless Commun.*, vol. 70, no. 10, pp. 6489-6502, Oct. 2022.
- [12] Bezdek, James C., and Richard J. Hathaway, "Convergence of alternating optimization," *Neur. Parallel Sci. Comput.*, 2003, pp. 351-368.
- [13] Tseng, Paul, "Convergence of a block coordinate descent method for non-differentiable minimization," J. Optim. Theory Appl., 2001, pp. 475-494
- [14] Beck, Amir, and Luba Tetruashvili, "On the convergence of block coordinate descent type methods," SIAM J. Optim., 2013, pp. 2037-2060.

- [15] Hong et al., "Iteration complexity analysis of block coordinate descent methods," Math. Program., 2017, pp. 85-114.
- [16] Z. -Q. Luo, W. -K. Ma, A. M. -C. So, Y. Ye and S. Zhang, "Semidefinite Relaxation of Quadratic Optimization Problems," *IEEE Signal Process Mag.*, vol. 27, no. 3, pp. 20-34, May 2010.
- [17] S. H. Low, "Convex Relaxation of Optimal Power FlowPart I: Formulations and Equivalence," *IEEE Trans. Control Netw. Syst.*, vol. 1, no. 1, pp. 15-27, Mar. 2014.
- [18] Q. Wu and R. Zhang, "Intelligent Reflecting Surface Enhanced Wireless Network via Joint Active and Passive Beamforming," *IEEE Trans. Wireless Commun.*, vol. 18, no. 11, pp. 5394-5409, Nov. 2019.
- [19] H. Guo, Y. -C. Liang, J. Chen and E. G. Larsson, "Weighted Sum-Rate Maximization for Reconfigurable Intelligent Surface Aided Wireless Networks," *IEEE Trans. Wireless Commun.*, vol. 19, no. 5, pp. 3064-3076, May 2020.
- [20] Q. Wu and R. Zhang, "Beamforming Optimization for Wireless Network Aided by Intelligent Reflecting Surface With Discrete Phase Shifts," *IEEE Trans. Wireless Commun.*, vol. 68, no. 3, pp. 1838-1851, March 2020.
- [21] D. Dampahalage, K. B. Shashika Manosha, N. Rajatheva and M. Latvaaho, "Intelligent Reflecting Surface Aided Vehicular Communications," GC Workshops, Taipei, Taiwan, 2020, pp. 1-6.
- [22] H. Sun, X. Chen, Q. Shi, M. Hong, X. Fu and N. D. Sidiropoulos, "Learning to optimize: training deep neural networks for interference management," *IEEE Trans. Signal Process.*, vol. 66, no. 20, pp. 5438-5453, Oct. 2018.
- [23] L. Liang, H. Ye, G. Yu and G. Y. Li, "Deep-Learning-Based Wireless Resource Allocation With Application to Vehicular Networks," in *Proc. IEEE*, vol. 108, no. 2, pp. 341-356, Feb. 2020.
- [24] Z. Gao, M. Eisen and A. Ribeiro, "Resource Allocation via Model-Free Deep Learning in Free Space Optical Communications," *IEEE Trans. Wireless Commun.*, vol. 70, no. 2, pp. 920-934, Feb. 2022.
- [25] Ali Mehrabian, Vincent W. S. Wong, "Joint spectrum, precoding, and phase shifts design for RIS-aided multiuser MIMO THz systems", accepted for publication in proc. IEEE Trans. Commun., 2024.
- [26] Alexandropoulos, G. C., Samarakoon, S., Bennis, M., & Debbah, M., "Phase configuration learning in wireless networks with multiple reconfigurable intelligent surfaces", in *Proc. IEEE Workshop Global Commun. Conf.*, Dec. 2020.
- [27] C. Huang, G. C. Alexandropoulos, C. Yuen, and M. Debbah, "Indoor signal focusing with deep learning designed reconfigurable intelligent surfaces," in *Proc. IEEE Int. Workshop Signal Process. Adv. Wireless Commun.*, Cannes, France, Jul. 2019.
- [28] J. Gao, C. Zhong, X. Chen, H. Lin and Z. Zhang, "Unsupervised Learning for Passive Beamforming," *IEEE Commun. Lett.*, vol. 24, no. 5, pp. 1052-1056, May 2020.
- [29] T. Jiang, H. V. Cheng, and W. Yu, "Learning to reflect and to beamform for intelligent reflecting surface with implicit channel estimation," *IEEE J. Sel. Areas Commun.*, vol. 39, no. 7, pp. 1931-1945, May 2021.
- [30] Chen et al., "A Distributed Machine Learning-Based Approach for IRS-Enhanced Cell-Free MIMO Networks," [Online]. Available: https://doi.org/10.48550/arXiv.2301.08077.
- [31] W. Xia, G. Zheng, Y. Zhu, J. Zhang, J. Wang and A. P. Petropulu, "A Deep Learning Framework for Optimization of MISO Downlink Beamforming," *IEEE Trans. Commun.*, vol. 68, no. 3, pp. 1866-1880, Mar. 2020.
- [32] E. Björnson, M. Bengtsson, and B. Ottersten, "Optimal multiuser transmit beamforming: A difficult problem with a simple solution structure," *IEEE Signal Process Mag.*, vol. 31, no. 4, pp. 142-148, Jul. 2014.
- [33] J. Kim, H. Lee, S. -E. Hong and S. -H. Park, "Deep Learning Methods for Universal MISO Beamforming," *IEEE Wireless Commun. Lett.*, vol. 9, no. 11, pp. 1894-1898, Nov. 2020.
- [34] J. Kim, H. Lee, S. -E. Hong and S. -H. Park, "A Bipartite Graph Neural Network Approach for Scalable Beamforming Optimization," *IEEE Trans. Wireless Commun.*, vol. 22, no. 1, pp. 333-347, Jan. 2023.
- [35] M. Zhang, J. Gao and C. Zhong, "A Deep Learning-Based Framework for Low Complexity Multiuser MIMO Precoding Design," *IEEE Trans. Wireless Commun.*, vol. 21, no. 12, pp. 11193-11206, Dec. 2022.
- [36] W. Jin, J. Zhang, C. -K. Wen, S. Jin, X. Li, and S. Han, "Low-Complexity Joint Beamforming for RIS-Assisted MU-MISO Systems Based on Model-Driven Deep Learning," in *IEEE Trans. Commun.*, vol. 23, no. 7, pp. 6968-6982, July 2024.
- [37] J. Zhu, Y. Huang, J. Wang, K. Navaie, and Z. Ding, "Power efficient IRS-assisted NOMA," *IEEE Trans. Wireless Commun.*, vol. 69, no. 2, pp. 900-913, Feb. 2021.
- [38] G. Zhou, C. Pan, H. Ren, K. Wang, and A. Nallanathan, "Intelligent reflecting surface aided multigroup multicast MISO communication systems," *IEEE Trans. Signal Process.*, vol. 68, pp. 3236-3251, Apr. 2020.

- [39] X. Jiang, A. Decurninge, K. Gopala, F. Kaltenberger, M. Guillaud, D. Slock and L. Deneire, "A framework for over-the-air reciprocity calibration for TDD massive MIMO systems," *IEEE Trans. Wireless Commun.*, vol. 17, no. 9, pp. 5975-5990, Sep. 2018.
- [40] J. Vieira, F. Rusek, O. Edfors, S. Malkowsky, L. Liu and F. Tufvesson, "Reciprocity calibration for massive MIMO: Proposal, modeling, and validation," *IEEE Trans. Wireless Commun.*, vol. 16, no. 5, pp. 3042-3056, May 2017.
- [41] J. Zhang, M. You, G. Zheng, I. Krikidis and L. Zhao, "Model-Driven Learning for Generic MIMO Downlink Beamforming With Uplink Channel Information," *IEEE J. Sel. Areas Commun.*, vol. 21, no. 4, pp. 2368-2382, April 2022.
- [42] C. Huang, G. C. Alexandropoulos, A. Zappone, C. Yuen and M. Debbah, "Deep learning for UL/DL channel calibration in generic massive MIMO systems," in *Proc. IEEE Int. Conf. Commun.*, Shanghai, China, May 2019, pp. 1-6.
- [43] K. Hornik, M. Stinchcombe, and H. White, "Multilayer feedforward networks are universal approximators," *Neural Netw.*, vol. 2, no. 5, pp. 359-366, Jul. 1989.
- [44] H. Wei, D. Wang, and X. Y ou, "Reciprocity of mutual coupling for TDD massive MIMO systems," in *Proc. Int. Conf. Wireless Commun. Signal Process.*, Nanjing, China, Oct. 2015, pp. 15.
- [45] Y. Xu et al., "A block coordinate descent method for regularized multiconvex optimization with applications to nonnegative tensor factorization and completion," SIAM J. Imag. Sci., vol. 6, no. 3, pp. 1758-1789, 2013.
- [46] Q. Shi, M. Razaviyayn, Z. Luo, and C. He, "An iteratively weighted MMSE approach to distributed sum-utility maximization for a MIMO interfering broadcast channel," *IEEE Trans. Signal Process.*, vol. 59, no. 9, pp. 4331-4340, Sept. 2011.
- [47] N. Boumal, B. Mishra, P. -A. Absil, and R. Sepulchre, "Manopt, a Matlab toolbox for optimization on manifolds," *J. Mach. Learn. Res.*, vol. 15,no. 1, pp. 1455-1459, 2014.
- [48] E. Björnson and L. Sanguinetti, "Rayleigh fading modeling and channel hardening for reconfigurable intelligent surfaces," *IEEE Wireless Commun. Lett.*, vol. 10, no. 4, pp. 830-834, April 2021.
- [49] M. Abadi et al., "TensorFlow: Large-scale machine learning on heterogeneous systems," 2015, software available from tensorflow.org. [Online]. Available: https://www.tensorflow.org/
- [50] D. Kingma and J. Ba, "Adam: A method for stochastic optimization," Proc. Int. Conf. Learn. Represent. (ICLR), pp. 115, 2015.
- [51] F. Rusek et al., "Scaling up MIMO: opportunities and challenges with very large arrays," *IEEE Signal Process. Mag.*, vol. 30, pp. 4060, Jan. 2013.
- [52] I. Zakia, "Maximizing the Sum Rate of Massive MIMO with Rectangular Planar Array and MRT Beamforming," in 2019 IEEE 89th Vehicular Technology Conference (VTC2019-Spring), pp. 1-5, doi: 10.1109/VTC-Spring.2019.8746334.
- [53] H. Alwazani, A. Kammoun, A. Chaaban, M. Debbah, and M.-S. Alouini, "Intelligent reflecting surface-assisted multi-user MISO communication: Channel estimation and beamforming design," *IEEE Open J. Commun.*, Soc., vol. 1, pp. 661-680, May 2020.
- [54] J. Chen et al., "Channel estimation for reconfigurable intelligent surface aided multi-user mmWave MIMO systems," *IEEE Trans. Wireless Commun.*, vol. 22, no. 10, pp. 6853-6869, Oct. 2023.



RuiHua Zhang xxx



Gan Zheng (S'05-M'09-SM'12-F'21) received the BEng and the MEng from Tianjin University, Tianjin, China, in 2002 and 2004, respectively, both in Electronic and Information Engineering, and the PhD degree in Electrical and Electronic Engineering from The University of Hong Kong in 2008. He scurrently Professor in Connected Systems in the School of Engineering, University of Warwick, UK. His research interests include machine learning for wireless communications, reconfigurable intelligent surface, UAV communications and edge computing.

He is the first recipient for the 2013 IEEE Signal Processing Letters Best Paper Award, and he also received 2015 GLOBECOM Best Paper Award, and 2018 IEEE Technical Committee on Green Communications & Computing Best Paper Award. He was listed as a Highly Cited Researcher by Thomson Reuters/Clarivate Analytics in 2019. He currently serves as an Associate Editor for IEEE Wireless Communications Letters and IEEE Transactions on Communications



Kai-Kit Wong (M'01-SM'08-F'16) received the BEng, the MPhil, and the PhD degrees, all in Electrical and Electronic Engineering, from the Hong Kong University of Science and Technology, Hong Kong, in 1996, 1998, and 2001, respectively. After graduation, he took up academic and research positions at the University of Hong Kong, Lucent Technologies, Bell-Labs, Holmdel, the Smart Antennas Research Group of Stanford University, and the University of Hull, UK. He is Chair in Wireless Communications at the Department of Electronic and Electrical Engi-

neering, University College London, UK. His current research centers around 6G and beyond mobile communications. He is Fellow of IEEE and IET. He served as the Editor-in-Chief for IEEE Wireless Communications Letters between 2020 and 2023.



Kai Liang received the Ph.D. degree from the School of Telecommunications Engineering, Xidian University, China, in 2016. During 2014-2015, he visited the Network Convergence Laboratory, University of Essex, U.K., on the funds from the Program of the China Scholarships Council. He is currently an associate professor with the School of Telecommunications Engineering, Xidian University. He manages research projects funded by various sources such as NSFC, and the National Key R&D Program of China. His current research interests

include network slicing, beamforming design for MIMO system, simultaneous wireless information and power transfer, and digital twins.